



Article

Excellent Thermal and Dielectric Properties of Hexagonal Boron Nitride/Phenolic Resin Bulk Composite Material for Heatsink Applications

Egor A. Danilov ¹, Vladimir M. SamoiloV ^{1,2}, Innokenty M. Kaplan ^{1,2}, Elena V. Medvedeva ³, Andrey A. Stepashkin ⁴ and Victor V. Tcherdyntsev ^{4,*}

- ¹ Research Institute for Graphite-Based Structural Materials “NIIgrafit” (JSC “NIIgrafit”), Elektrodnyaya Street 2, 111524 Moscow, Russia; danilovegor1@gmail.com (E.A.D.); vsamoilov54@gmail.com (V.M.S.); kaplan.graphit@yandex.ru (I.M.K.)
- ² Federal State Budgetary Educational Institution of Higher Education “MIREA—Russian Technological University”, 119454 Moscow, Russia
- ³ Moscow Aviation Institute, Volokolamsk sh., 4, 125993 Moscow, Russia; lena_p@bk.ru
- ⁴ Laboratory of Functional Polymer Materials, National University of Science and Technology “MISIS”, Leninskii Prosp, 4-1, 119049 Moscow, Russia; a.stepashkin@misis.ru
- * Correspondence: vvch@misis.ru; Tel.: +7-910-400-2369

Abstract: In the present paper, we report polymer composites based on phenolic resin filled with hexagonal boron nitride; hot compression molding coupled with solution-based mixing were used to manufacture the composites. The paper presents experimental results on the physical and physico-chemical properties of the obtained composites: thermal stability in air and argon, dielectric constant and dielectric loss tangent, active electrical resistance, thermal conductivity (mean and anisotropy), and mechanical strength. It is shown that the proposed technique of composite manufacturing, including the application of high-process pressures, makes it possible to obtain materials with high anisotropy of thermal conductivity, extremely high-filler content, and excellent dielectric properties, all of which are very important for prospective highly efficient lightweight heatsink elements for electronic devices. Experimental values of thermal conductivity and dielectric constant were analyzed using known mathematical models. Experimental values for thermal conductivities (up to $18.5 \text{ W} \cdot \text{m}^{-1} \cdot \text{K}^{-1}$) of composites at filler loadings of 65–85 vol.% are significantly higher than published data for bulk boron nitride/polymer composites.

Keywords: heatsink materials; polymer-matrix composites; boron nitride; thermal properties; electrical properties; compression molding



Citation: Danilov, E.A.; SamoiloV, V.M.; Kaplan, I.M.; Medvedeva, E.V.; Stepashkin, A.A.; Tcherdyntsev, V.V. Excellent Thermal and Dielectric Properties of Hexagonal Boron Nitride/Phenolic Resin Bulk Composite Material for Heatsink Applications. *J. Compos. Sci.* **2023**, *7*, 291. <https://doi.org/10.3390/jcs7070291>

Academic Editor: Francesco Tornabene

Received: 31 May 2023
Revised: 4 July 2023
Accepted: 10 July 2023
Published: 14 July 2023



Copyright: © 2023 by the authors. Licensee MDPI, Basel, Switzerland. This article is an open access article distributed under the terms and conditions of the Creative Commons Attribution (CC BY) license (<https://creativecommons.org/licenses/by/4.0/>).

1. Introduction

Intensive growth of transistor-based computer chips in modern technology leads to an exponential increase in heat generation per unit area. Excessive heat generation leads to the formation of local overheated points (so called hotspots) on the surface of the chip, which results in incorrect electronics operation and eventual failure; therefore, it is necessary to create materials with high-thermal conductivity values, including thermal interface materials (TIMs), which can effectively dissipate heat to the environment or active cooling system, such as a radiator, heat pipe, or Peltier element. Air has extremely low-heat conductivity (ca. $0.024 \text{ W} \cdot \text{m}^{-1} \cdot \text{K}^{-1}$ [1]), and even with thorough mechanical finishing, the effective contact area at the chip-radiator interface is only about 1–3% [2]; heat flux is typically distributed ineffectively. Therefore, polymer-based TIMs are required to provide excellent mechanical contact in order to reduce thermal contact resistances between the chip and heatsink [1–7]. In order to improve heat removal from the surface of the radiator, heat dissipating materials with high-thermal conductivity are required.

Polymer-based materials are routinely used as TIMs; their use in heatsink applications, however, is limited due to low thermal conductivity (below $0.5 \text{ W}\cdot\text{m}^{-1}\cdot\text{K}^{-1}$) and insufficient strength, as compared to conventional metals [1–10]. Although great progress has been made recently in the field of highly conductive polymers [11], practically relevant values of several to tens $\text{W}\cdot\text{m}^{-1}\cdot\text{K}^{-1}$ have been achieved primarily for oriented films or fibers that cannot be directly applied to produce bulk heatsink articles. Therefore, polymer composite materials (PCMs), based on thermally conductive fillers, are far more extensively developed and applied in automotive radiators [12], finned heatsinks for electronics [13,14], and heat exchangers [15].

Although many fillers have been described as suitable for polymer composites-based heatsink materials [1–5,7,10,11], metallic and carbon nanoparticles are found to provide the highest thermal conductivity values. However, composites then become electrically conductive, which limits their applications in many electronic devices. In this respect, composites based on hexagonal boron nitride (h-BN) attract significant research interest due to their excellent dielectric properties and thermal conductivity; layered structure of h-BN provides high- and controlled property anisotropy; in addition, h-BN has superb thermal stability. The decomposition temperature of h-BN in vacuum reaches 3000 K, so respective composites are able to withstand operating temperatures limited only by decomposition temperature of the matrix material [16–21].

Another great advantage of h-BN is that its dielectric constant and electrical conductivity are close to those of pure polymers; therefore, h-BN-based materials can be used for heatsink applications in power electronics [17,19–29]. h-BN-based composites demonstrate highly effective thermal conductivity (k_{eff}), which is very important for microelectronics-related applications, where heat-dissipating systems are very limited in size. The in-plane thermal conductivity of the pure polycrystalline h-BN reaches $180\text{--}200 \text{ W}\cdot\text{m}^{-1}\cdot\text{K}^{-1}$ [4,8,10] (and even higher in thin films and microlamellae); therefore, effective thermal conductivity in composites is typically lower. In the present study, its value was taken as $100 \text{ W}\cdot\text{m}^{-1}\cdot\text{K}^{-1}$. Moreover, due to the layered structure of h-BN, it is possible to achieve controlled thermal conductivity anisotropy in the composites, that is, to be able to control heat flux dissipation throughout an electronic device. This reduces the probability that hotspots will result in critical chip overheating.

Epoxy resin was used as binder in most studies [16–19,22–25,30–32], since it is a thermoset polymer, and its bis-phenolic-based precursor (although naphthalene-type precursors were also considered [33]) has low viscosity, making the process of mixing the filler with matrix straightforward. For example, in the report by Wang et al. [30], h-BN/epoxy composite films were manufactured; electrical and thermal conductivity of the obtained samples reached the values of 3.0–3.5 for dielectric constant, 10^{-12} S/cm for electrical conductivity and $0.205 \text{ W}\cdot\text{m}^{-1}\cdot\text{K}^{-1}$ for thermal conductivity, respectively. These values cannot be used as a reference in the current study as they pertain to only 2 wt.% filler loading in film composite, whereas thermal conductivity should be much higher at filler loadings exceeding the percolation threshold. Several studies report thermoplastic polymers as matrices, i.e., polypropylene. Takanashi et al. [28] used injection molding and hot-press molding to achieve excellent dielectric properties (dielectric constant ~ 3.3 , dielectric loss tangent $\sim 2\cdot 10^{-4}$) at 40 vol.% filler content, but thermal conductivities were quite low ($2.1 \text{ W}\cdot\text{m}^{-1}\cdot\text{K}^{-1}$ for hot-press molded and below $0.4 \text{ W}\cdot\text{m}^{-1}\cdot\text{K}^{-1}$ for injection molded composite).

As can be readily seen from just the mentioned data, the level of thermal conductivity for h-BN-based composites is far below the values for polycrystalline h-BN, which is typical for all PCMs. This fact is generally attributed to local thermal resistances of the interparticle boundaries. In the case of poor adhesion, this can be due to filler particles agglomeration and intrinsic porosity of the agglomerates [32], whereas for strong filler-matrix interactions, particles primarily interact through non-conductive matrix layers, resulting in increased thermal resistance [31]. In the case of non-metallic fillers, the effect of strong phonon scattering on the interparticle boundaries also becomes important. Surface modification

and functionalization are often used in literature to improve local thermal resistances of the composites [4].

Various surface modifications of boron nitride particles, namely exfoliation in aromatic solvents, such as polysulfide-p-phenylene, poly-p-phenylene-vinylene [34,35], increase contact surface, as well as non-covalent functionalization [36,37], which does not provide PCMs with acceptable thermal properties. For example, functionalization resulted in thermal conductivity increase from 0.3 to 0.35 $\text{W}\cdot\text{m}^{-1}\cdot\text{K}^{-1}$ for PCM with 10% h-BN content [35]. It can be concluded that these types of modification of h-BN particles do not lead to a significant increase in the heat-conducting properties of PCMs.

Heat resistance and thermal properties of phenolic resins (PRs) are superior to most polymers, i.e., for epoxy resins, decomposition is significant already at 430 K, whereas PRs are stable up to 530 K, therefore they are more suitable for manufacturing materials for high-temperature applications. Due to the increased heat and fire resistance, as well as chemical stability, PR-based materials are used in applications that require excellent fire safety properties, i.e., in the production of power supply modules, aerospace components, vacuum devices [38,39]. Nevertheless, published data on PR-based, heat-conductive composites, including h-BN/PR-system, are scarce.

Other temperature-resistant polymers, such as polyetheretherketone (PEEK), have a significant disadvantage as compared to PRs; the processing temperatures are much higher, about 340 °C [40], whereas for polyetherketone ketone (PEKK), the temperatures are 320 to 380 °C [41]. In addition, the high-melt viscosity of these thermoplasts is a significant processing disadvantage as compared to PR.

Films based on h-BN are used as TIMs with dielectric properties in electronics. Bulk materials based on h-BN and PRs can be used as materials for heat exchangers and dimensionally stable structures. A lot of research [12–15] is conducted on bulk heatsink composites.

Dielectric properties of h-BN/PR systems are considered in detail by Ko et al. [42], where electrically insulating properties of PR-based composite and mixture of two heat-conducting fillers, h-BN and ZnO, were studied. PR was custom-made; nevertheless, thermal conductivity values were quite low (3.5 $\text{W}\cdot\text{m}^{-1}\cdot\text{K}^{-1}$ in-plane and only ca. 1.1 $\text{W}\cdot\text{m}^{-1}\cdot\text{K}^{-1}$ through-plane at 80 vol.% of filler). The use of PR-based solvent processing makes it possible to achieve high and ultra-high content of the heat-conducting filler in the composite, but post-processing conditions (drying, pre-mixed powder preparation, molding) apparently define the thermophysical characteristics of the resulting material.

In the present paper, the influence of h-BN content on thermal conductivity, thermal stability and electrophysical characteristics (dielectric constant, dielectric loss tangent, electrical conductivity) of hot-pressed compositions of the h-BN/PR composites were studied. Filler concentration correlations of thermal conductivity and dielectric constants were described using known physical models. The adequacy of the isolated medium and effective medium models for the description of h-BN/PR systems was analyzed.

2. Materials and Methods

2.1. Manufacturing of h-BN/PR Composites

Dissolution of PR (novolak-type, grade SF-012A, GOST 18694-2017, Metadinea, Orekhovo-Zuyevo, Russia) in isopropyl alcohol (IPA) (99.5+%, ECOS-1, Staraya Kupavna, Russia) was carried out at 310–330 K using magnetic stirrer (~200 rpm) (C-MAG HS-7, IKA, Staufen, Germany); the resulting solution of PR in IPA was mixed with filler particles (h-BN, 97.6+%, UNIKHIM, Ekaterinburg, Russia) followed by evaporation of alcohol under vacuum at 350 K. Dried mixtures were milled in IVT-3 bowl vibrating pulverizer (Mechanobrtehnika, Saint-Petersburg, Russia) for 60 s in order to obtain homogeneous moldable powders; resulting composites were obtained by the hot-molding (pressing) method using a PSU-10 hydraulic press (maximal load 100 KN, Techmash, Neftekamsk, Russia), by applying 40–80 MPa pressure at 180 °C for 60–90 min.

2.2. Characterization Techniques

Particle size distributions of h-BN particles were measured via the laser diffraction technique of aqueous suspensions (6 mg/mL, 15 min. ultrasonication), using SYNC setup with the FLOWSYNC (both Microtrack MRB, Montgomeryville, PA, USA) module for measuring suspensions. Mie theory was used to calculate distributions.

Scanning electron microscopy (SEM) studies were performed using a Thermo Fisher Prisma E instrument (Waltham, MA, USA), operating at 10.0 kV accelerating voltage with no metallization of the samples.

Measurements of thermal conductivities were carried out by steady-state heat flux method at temperature range of 293–303 K (ASTM C5470-17 method) in the direction of the molding axis (through-plane, k_z), as well as in a perpendicular direction (in-plane, k_x).

Thermogravimetric analysis (TGA) was performed on the Jupiter F1 STA unit (TGA/DSC) (Netzsch, Selb, Germany), using sapphire crucibles and standards; nitrogen (99.999 +%) was used for inert atmosphere, whereas dried air was used as an oxidizing agent; heating rate was 5 K/min in all cases.

Relative dielectric permittivity (dielectric constant, ϵ_r) and dielectric loss tangent ($\tan \delta$) were evaluated using an E4990a impedance analyzer (frequency range 1 Hz–30 MHz, Keysight, Santa-Rosa, CA, USA) with 16451B dielectric test fixture (Keysight, Santa-Rosa, CA, USA); measurements were carried out according to ASTM D150-18 standard.

Active resistance and electrical conductivity were measured using a T0mM-01 teraohmmeter (10^6 – 10^{15} Ω range, NPP Norma, Samara, Russia), at a voltage of 100 V.

Compressive strength measurements were carried out using a Z250 unit (Zwick Roell AG, Fürstenfeld, Austria), following ASTM D6641/D6641M-16e1 route at 0.2 mm/min. loading speed.

3. Results and Discussion

3.1. Filler Particle Size Distribution

Analysis of the published data showed that, for h-BN-based composites, the higher the initial particle size of the filler, the higher the maximal thermal conductivity in the composite [31,43]. This inverse proportionality between thermal conductivity and particle size can be explained by the fact that h-BN interparticle heat transfer is ballistic in nature, that is, heat transfer between the boundaries of neighboring particles [24] becomes less effective as the relative concentration of the edge atoms increases, whereas the average interparticle contact area decreases. Therefore, no preliminary grinding of the filler was used in the present work.

Particle size distribution for h-BN used in the present study, as determined via laser diffraction, is depicted on Figure 1a. Distribution is clearly bi-modal with only a small fraction of particles having a size above 20 μm . Average particle size of h-BN was 5.3 μm (leftmost peak in Figure 1a).

Results of laser diffraction measurements are further supported by SEM studies. h-BN particles have a typical, layered structure and size in the range of 5–15 μm , which is very similar to natural graphite.

3.2. h-BN/PR Composites Manufacturing Technology

The step-by-step scheme for manufacturing h-BN/PR composites is shown in Figure 2. We used the matrix dissolution method in order to obtain ultra-high volumetric filler content (up to 85%), which is extremely important to achieve maximal thermal conductivity values, i.e., values of up to $30.25 \text{ W}\cdot\text{m}^{-1}\cdot\text{K}^{-1}$, which were achieved in thin oriented composite papers (h-BN-based nanosheets/cellulose nanofibers) at 70 wt.% h-BN loading [44]; similarly, high values were achieved for highly filled PVA-based films by Song et al. [45], but this level of thermal conductivities was never reported for bulk composites, as it is very difficult to achieve particle orientation, i.e., avoiding agglomeration and porosity that lead to significant deterioration of thermal properties. Therefore, most of the published data for

bulk composites report modest thermal conductivity values of $0.6\text{--}10\text{ W}\cdot\text{m}^{-1}\text{ K}^{-1}$ at filler loadings that are typically under 25 vol.% [46].

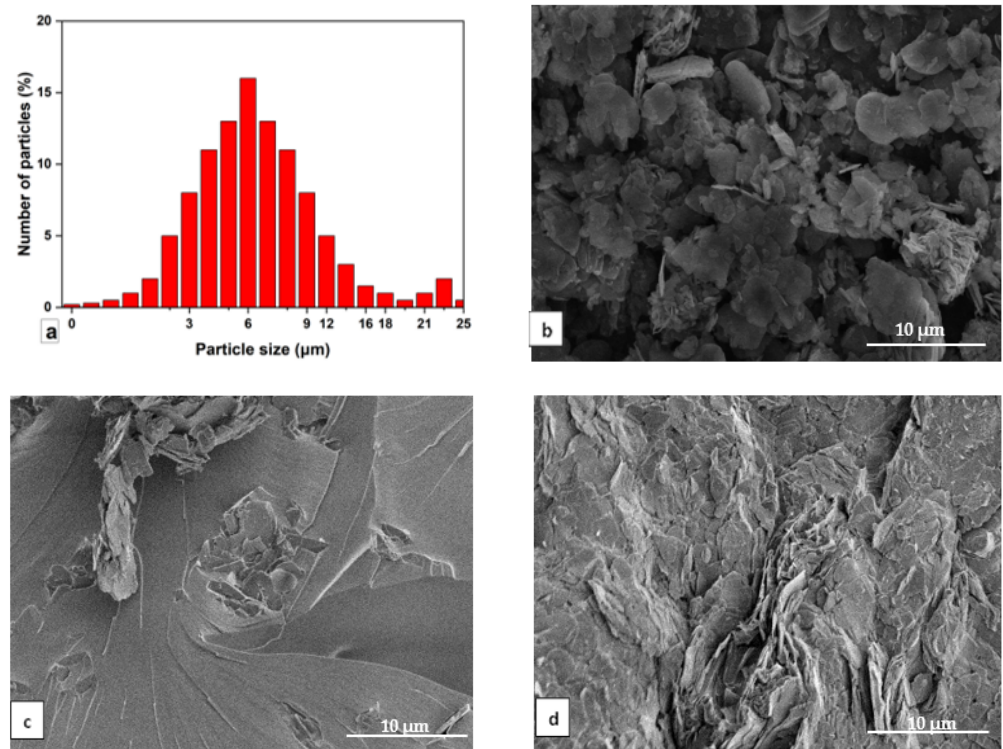


Figure 1. h-BN characterization: (a) volumetric particle size distribution, (b–d) low-magnification SEM image 5, 85% vol. h-BN, neat h-BN.

We further used vibration grinding to obtain homogeneous powders, which is crucial for high-quality molding. Another advantage of this technique is that the grinding mechanism primarily features shear and interparticle collisions, which ensures that resin is evenly distributed throughout both the mixture (macroscopically) and on particles’ surfaces (microscopically, see Figure 1c,d).

As can be readily seen from the sample images on Figure 2, incorrect pressure (too high in this case) leads to visually observable horizontal fractures.

Hot molding is widely used for PR-based composites. In the case of h-BN-based composites, it was shown that the application of pressure is clearly advantageous for thermal conductivity, in order to minimize porosity (Figure 3a) and ensure strong bonding of the composite (Figure 1c,d). Recently, Moradi et al. [32] showed that by applying only 2 MPa while curing h-BN/epoxy composite, one can increase thermal conductivity twofold. Another consideration in favor of hot molding is moderate particle orientation, sufficient for increased material anisotropy, yet not as high as to prevent effective contacts of layered particles [4,47].

Theoretical density was calculated using the following formula based on the simple rule of mixtures (1):

$$\rho_{theor.} = (1 - V_f) \cdot \rho_m + V_f \cdot \rho_f \tag{1}$$

where ρ_m —density of matrix (1.20 g/cm^3), and ρ_f —density of filler (2.10 g/cm^3).

Porosity ϕ was calculated using the following Formula (2):

$$\phi = \frac{\rho_{theor.} - \rho_{experim.}}{\rho_{theor.}} \cdot 100\% \tag{2}$$

$\rho_{experim.}$ being experimental value for bulk density.

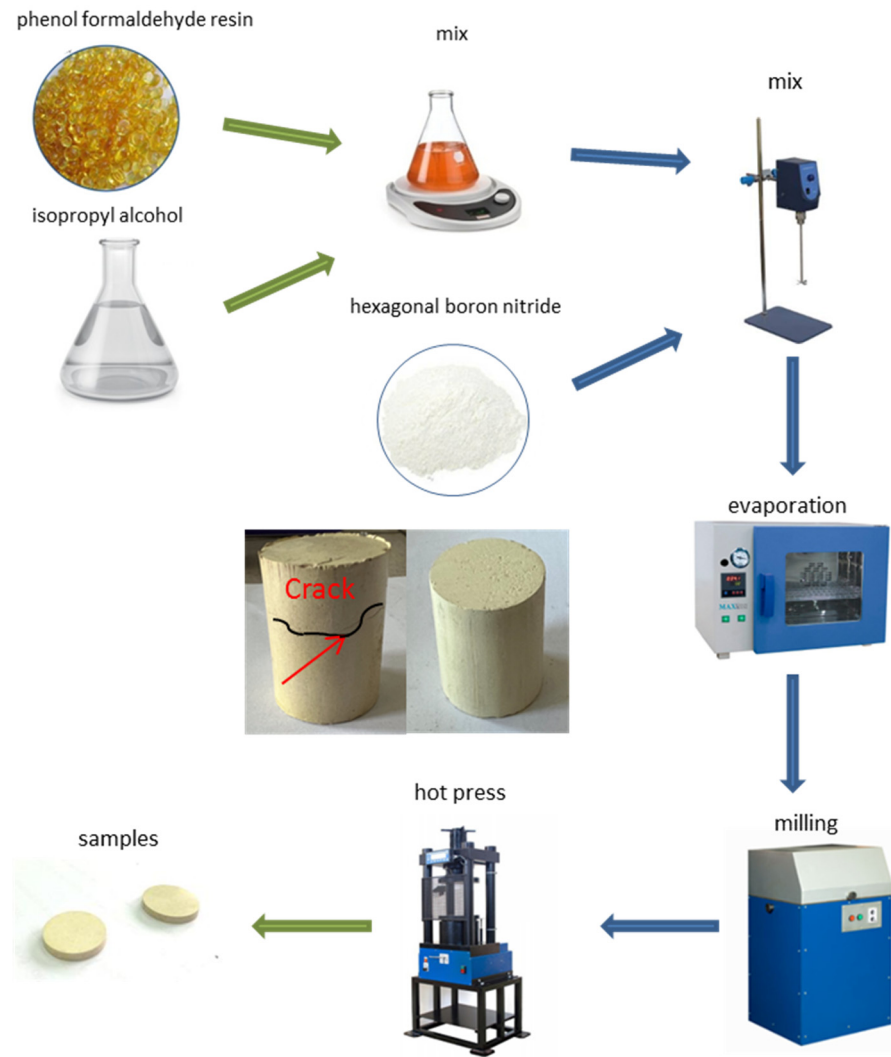


Figure 2. Process scheme for manufacturing h-BN/PR bulk composites.

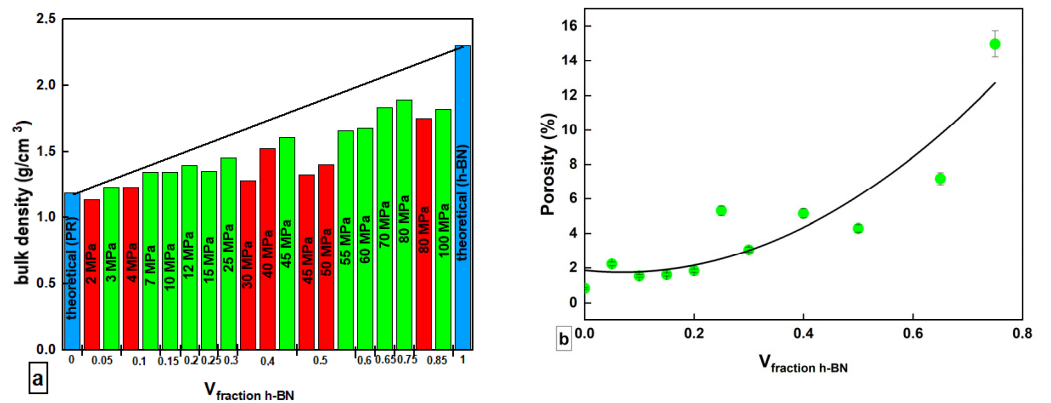


Figure 3. Dependence of (a) bulk density upon molding pressure, and (b) porosity upon filler loading.

Figure 3a shows the plot of experimental values for bulk density vs. theoretical density, as defined by Equation (1). It can be readily seen from the data that, in addition to great pressure leading to the formation of cracks in the composite, there is also a threshold value for each filler fraction that allows for manufacturing the composite with minimal porosity (compare the green and orange bars). This fact may be due to increased intrinsic porosity at low molding pressures.

As a result of using significant processing pressures (40–80 MPa), composites with densities close to theoretical (porosity below 6–7 vol.%) and up to very high-filler loadings (about 75–80 vol.%) were obtained. Increased porosity (above 10 vol.%) is only seen with loadings as high as 85 vol.% (see Figure 3b), which may be attributed to technique’s inability to provide sufficient matrix polymer distribution at high-filler fractions. This is very beneficial, as the presence of pores greatly reduces thermal conductivity of the material (see Figure 4a).

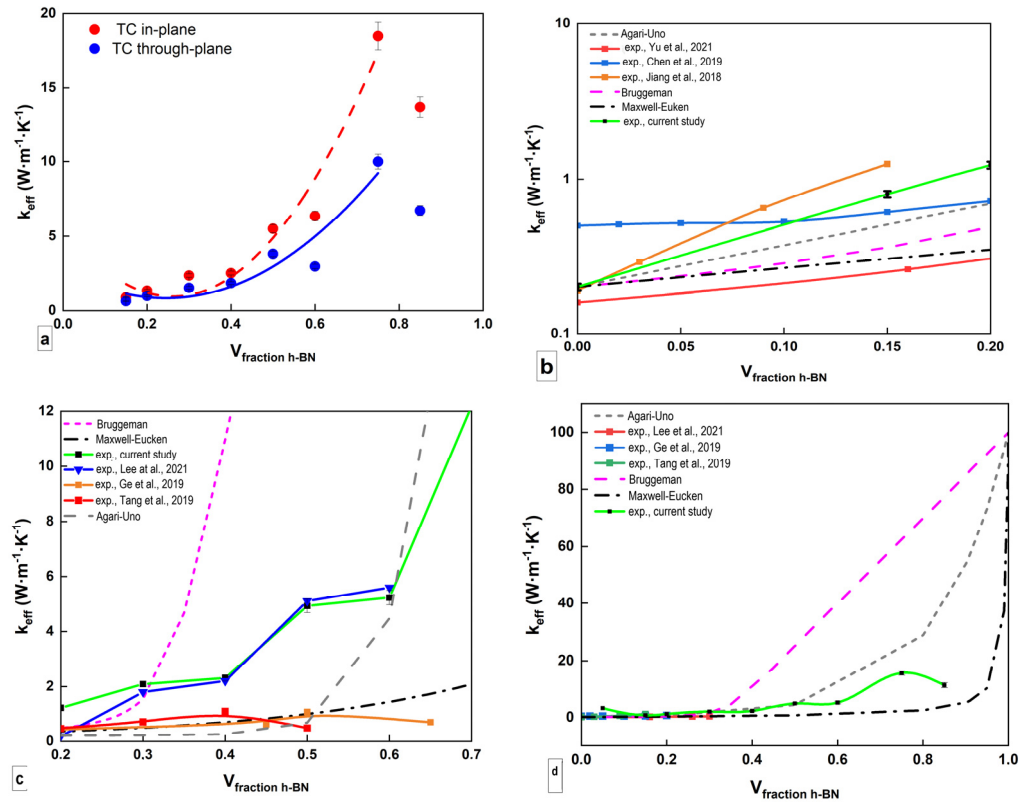


Figure 4. Thermal conductivity of h-BN/PR composites. (a) experimental data for k_x (●) and k_z (○), (b–d) calculated k_{eff} values vs. known theoretical models and other experimental works [48–53].

In this work, samples of heat-conducting h-BN/PR composites were obtained with filler loadings in the range of 5 to 85 vol.% and high homogeneity.

3.3. Thermal Conductivity Analysis

In several recent studies, thermal and dielectric properties of h-BN/polymer composites, such as thermal conductivity, dielectric permittivity, and dielectric loss tangent have been assessed thoroughly, and frequency-dependent dielectric characteristics were studied in detail [17,19–29]. The issue of anisotropy influence on thermal properties of the composites has been addressed as well [30,48].

The issue of heat-conducting properties of h-BN based compositions has had considerable attention in several studies [16,18–21,24,28–32,42–47,54]. Unfortunately, reported values of effective thermal conductivity were insufficient (no higher than $2.0 \text{ W}\cdot\text{m}^{-1}\cdot\text{K}^{-1}$), since composites with relatively low-filler contents were obtained.

Gu et al. [55] described dielectric heat-conducting composite materials, based on boron nitride and polyimide, were obtained by hot pressing. The thermal conductivity of PCM is $0.696 \text{ W}\cdot\text{m}^{-1}\cdot\text{K}^{-1}$, and the dielectric constant is 3.77 with a mass content of filler of 30%. In the work [56], PCMs based on thiol-epoxy elastomers and micron-sized boron nitride were synthesized by in situ polymerization; a filler of 17.5 wt.% achieved thermal conductivity of $2.4 \text{ W}\cdot\text{m}^{-1}\cdot\text{K}^{-1}$; surface activation and the creation of tubes similar to carbon nanotubes based on boron nitride does not lead to a noticeable improvement in the heat-conducting

properties of the material. In a number of recent works [57,58], PCMs were obtained based on plastics with carbon fillers, such as graphite and graphene; this class of materials does not have the dielectric characteristics necessary for use as heat-dissipating components in microelectronics [59]. PCMs based on polydopamine and boron nitride with a filler content of 17.5 wt % were obtained, and thermal conductivity of $2.4 \text{ W}\cdot\text{m}^{-1}\cdot\text{K}^{-1}$ was achieved.

Nevertheless, despite the wide scatter of the data obtained and insufficient thermal properties of most of the obtained PCMs, in a number of works, researchers were able to manufacture PCMs with high-thermal conductivity; for example, in the work by Novokshonova et al. [60], thermal conductivity of $27.6 \text{ W}\cdot\text{m}^{-1}\cdot\text{K}^{-1}$ was achieved at a filler content of 95 wt %. The thermal conductivity value of $12.5 \text{ W}\cdot\text{m}^{-1}\cdot\text{K}^{-1}$ was reported at a filler content of 65 wt % [61]. PCM, based on cellulose fibers and boron nitride nanotubes, achieved a thermal conductivity of $22 \text{ W}\cdot\text{m}^{-1}\cdot\text{K}^{-1}$ [37].

As can be readily seen from Figure 4a, all composites demonstrated significant anisotropy of thermal conductivity, which may be due to preferential orientation of filler particles. In-plane thermal conductivity k_x reaches very high values of $18.5 \text{ W}\cdot\text{m}^{-1}\cdot\text{K}^{-1}$ at 75 vol.%, and the k_x/k_z ratio is 1.5–2.2 (for 5 and 85 vol.%, respectively). Anisotropy makes it possible to create a predefined structure for preferential heat removal in the heatsink system. We further used effective thermal conductivity k_{eff} , defined by simple averaging over three main axes of a transverse-orthotropic body (3), as a figure of merit for thermal conductivity:

$$k_{eff} = \frac{2k_x + k_z}{3}, \tag{3}$$

Experimental values were compared with three models that are most suitable for describing thermal conductivity in polymer composites. Thermal conductivity of pure h-BN was taken to be $100 \text{ W}\cdot\text{m}^{-1}\cdot\text{K}^{-1}$ (taking into account possible local contact resistances), whereas thermal conductivity of the PR was $0.25 \text{ W}\cdot\text{m}^{-1}\cdot\text{K}^{-1}$ [42]. Thermal conductivity of composites is a property that is difficult to describe adequately, since there may be substantial differences in the properties of components, i.e., 400 times in this case.

Historically, the first group of models used an approximation of the isolated medium [62], that is, particles of heat-conducting filler are considered as non-interacting homogeneous spheres in a homogeneous polymer medium. These models have a high accuracy for regularly shaped particles at low filler content (less than 20–30 vol.%), and account for small differences in the thermal conductivity of the matrix and filler. The first proposed model to use this approximation was the Maxwell–Eucken model [62] (4):

$$k_{eff} = k_m \frac{k_f + 2k_m + 2V_f(k_f - k_m)}{k_f + 2k_m - V_f(k_f - k_m)}, \tag{4}$$

k_m —thermal conductivity of matrix,

k_f —thermal conductivity of filler,

V_f —filler volume content.

It is clearly seen from Figure 4b–f that this model provides significantly lower estimates and is not adequate in all of the studied concentration range, which might indicate that interparticle interactions and property differences play their significant role, even at lower filler loadings (see Figure 4b).

Second, more modern groups of models use effective medium approximation (EMA); the first model of this type was proposed by Bruggeman (5) [63,64]. It is applicable in the case of particles with complex shapes, for example, layered structures, fibers, etc.; its main advantage is that interparticle contacts can be taken into account. In addition, it has been reported to provide a higher accuracy, even beyond the percolation threshold.

$$V_m \frac{k_m - k_{eff}}{k_m + 2k_{eff}} + V_f \frac{k_f - k_{eff}}{k_f + 2k_{eff}} = 0. \tag{5}$$

For the reported data, the Bruggeman model is much more accurate than Maxwell–Eucken (4) at lower and medium loadings (up to 30 vol.%, see Figure 4b), but provides significant overestimates at higher concentrations (Figure 4c,d). Apparently, local contact thermal resistances (with possible re-agglomeration) dominate at higher concentrations, and should also be taken into account.

In addition to the Bruggeman model, the semi-empirical Agari–Uno model (6) is widely used to describe composites based on metal particles, graphite, and ceramics [65,66]. It accurately describes the thermal conductivity of materials with high- and ultra-high filler content, including highly anisotropic fillers. We set the empirical coefficients as $C_1 = 0.7$, $C_2 = 1$ as the best fit through zero and 100 vol.% points:

$$\log(k_{eff}) = V_f C_2 \log(k_f) + (1 - V_f) \log(C_1 k_m), \quad (6)$$

The Agari–Uno model seems to best describe experimental data (see Figure 4d–f), but definitive structural conclusions cannot be drawn from it, except that $C_2 \geq 1$ means that the filler is very prone to forming conduction paths throughout polymer matrix in this particular system, and conductivity is defined not by polymer crystallization and orientation in the presence of filler, but by the formation and structure of these conductive paths. It can be seen that deviations are greatest in the middle of concentration range (20–60 vol.%) above the percolation threshold but before the dominating influence of the filler thermal conductivity.

3.4. Thermogravimetric Analysis and Thermal Stability

Thermogravimetric method is widely used to evaluate degradation temperatures of polymer-based compounds. We used a temperature range of 300–1250 K for each composition and then estimated its degradation temperature as corresponding to a 2% weight loss. Figure 5a shows concentration curves for as-defined degradation temperature. While degradation temperatures monotonously increase with filler loading, stability in the air for low and medium loadings is surprisingly even and slightly higher than in the inert atmosphere at 75 and 85 vol.% stability in the air. However, decreases may be attributed to increased porosity. In any case, for high-filler loadings, temperature stability reaches 600–800 K, which makes these composites suitable for power electronics and applications with substantial fire safety requirements.

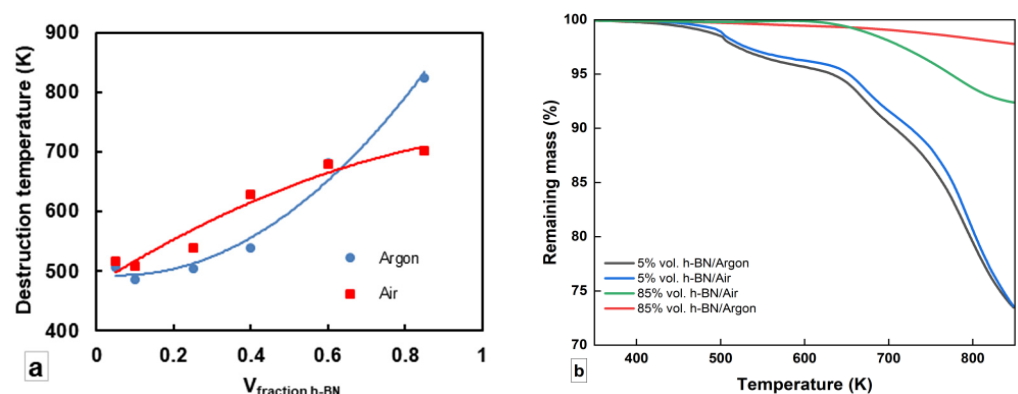


Figure 5. Thermogravimetric analysis of h-BN/PR composites. (a) dependence of composite degradation temperature on filler loading, and (b) thermogravimetric curves for 85% and 5% h-BN-containing composites in argon and air.

Figure 5b compares the thermogravimetric curves in the air, argon 5 and 85 vol.% composites. It can be readily seen that the 85 vol.% h-BN composite is far more thermally stable; therefore, it is highly desirable to use composites with higher filler content for high-temperature applications. Therefore, it is obvious that this technology for obtaining

PCM h-BN/PRs makes it possible to obtain TIM with an operating temperature of at least 480 K.

3.5. Dielectric Properties

Frequency range 1 KHz to 1 MHz was used for ϵ_r and $\tan \delta$ measurements; 1 MHz was taken as the reference frequency for concentration correlations. Figure 6a shows that ϵ_r values vary in the range from 4.2 to 5.5 and even slightly decrease at higher loadings. This is explained by the fact that boron nitride has an extremely low dielectric constant: $\epsilon_{r, h-BN}$ in the plane of the particle is 6 to 6.5, in the through-plane direction 2.8 to 3.8; whereas for the PR, ϵ_r is in the range of 3.5–4.5 [17,19,67]. In addition, composite ϵ_r value also depends on the boundary and contact phenomena, as well as porosity. As can be seen, at such close values for the filler and matrix, ϵ_r appears to be following the simple rule of mixtures (Figure 6a). Maxwell–Garnett isolated media model for dielectric constant (7) [68] matches experimental data only slightly better.

$$\epsilon_r = \epsilon_m \frac{\epsilon_f + \epsilon_m + 2V_f(\epsilon_f - \epsilon_m)}{\epsilon_f + 2\epsilon_m - V_f(\epsilon_f - \epsilon_m)}, \tag{7}$$

ϵ_f, ϵ_m —dielectric constants for filler and matrix respectively.

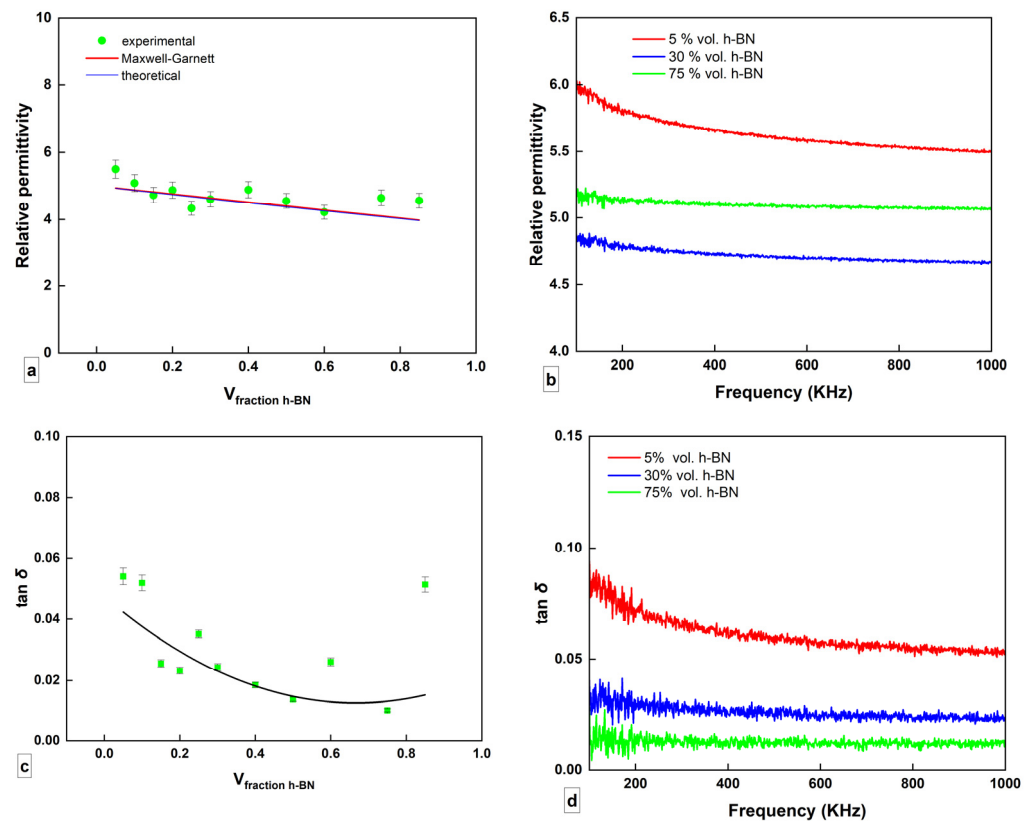


Figure 6. Dielectric properties of h-BN/PR composites: (a) ϵ_r —filler loading plot (frequency 1 MHz), (b) ϵ_r —frequency plot (5, 30, 75 vol.%), (c) $\tan \delta$ —filler loading plot (frequency 1 MHz), (d) $\tan \delta$ —frequency plot (5, 30, 75 vol.%).

Figure 6b demonstrates that ϵ_r ranges from 4.6 to 5.6 at 30 vol.% filler content for frequencies of 8–1000 KHz; therefore, the frequency plot is highly stable. Figure 5c shows that $\tan \delta$ at 1 MHz varies with filler loading from 0.015 to 0.055, which corresponds to an angle change from 0.8 to 3.2, showing a slight minimum at 50 vol.%, which may once again be linked with an increased influence of contact phenomena and porosity at higher

filler loadings. The low value of $\tan \delta$ and weak frequency dependence are important for dielectrics used in high-frequency applications, i.e., 5G. On the other hand, $\tan \delta$ is a structurally dependent property, especially for composites, so its relatively low values for a given polymer may be used as a sign of well-structured dielectric material.

Figure 6d shows the $\tan \delta$ -frequency plot for the 30 vol.% composite. From 20 KHz upwards, $\tan \delta$ is almost constant (around 0.05). Through analyzing the plots, we can conclude that, in the entire range of filler loadings, both ϵ_r and $\tan \delta$ values meet the requirements usually posed on industrial dielectrics ($\epsilon \sim 2$ to 8, $\tan \delta < 10^{-1}$), although the scatter in the experimental data is significant. The current study was not able to measure the anisotropy of the dielectric properties; therefore, it is logical to assume that, on the one hand, concentration correlations should generally follow the same trends as for thermal conductivity due to orientation of the filler particles, but on the other hand, one should not expect significant differences for axial and radial directions, as ϵ_r for h-BN and PR are very close, as can be readily seen from Figure 6a.

It should also be noted that the studied range frequency plots for the real part of ϵ_r and $\tan \delta$ behave symbotically. Although further research might clarify the nature of refraction and reflection properties in the studied composites, one can qualitatively state that in the h-BN/PR system at low frequencies, the well-known Kramers–Kronig dispersion equations take hold, and the system shows no non-linear effects [69].

Much research has been carried out to implement h-BN-based materials and nanostructures in nanoelectronic devices [70]. In the present case, used frequencies were too low to establish any significant electronic effects, which is due to the wide bandgap in h-BN. Nevertheless, the assessment of near-optical and THz frequency areas might reveal potentially interesting effects for the system under study.

Evaluation of specific electrical resistance and electrical conductivity was performed using the 2-probe technique and a teraohmmeter. Figure 7 shows that all h-BN/PR composites have sufficient electrical resistance ($\gg 10 \text{ M}\Omega \cdot \text{cm}$), so all of them are sufficiently reliable dielectrics to ensure static discharge or short circuit safety.

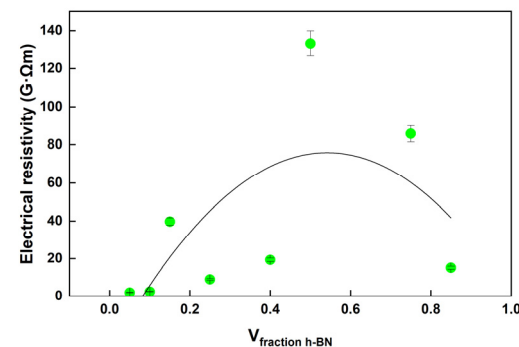


Figure 7. Dependence of the specific electrical resistivity of composites on filler loading.

The plots show the constant increase of electrical resistivity with increased filler loading, again supporting the need to use composites above 40 vol.% filler content, in order to achieve higher level of both thermal and electrical properties.

3.6. Mechanical Properties

Composites for heatsink application should withstand mechanical stress in order to be machined into finned radiators, heat exchangers, etc. Generally, the accepted level of mechanical strength for the material to be processed by most machining techniques (cutting, milling cutting, drilling, polishing) is over 20 MPa. Stress–strain curves at compression for several filler loadings are depicted in Figure 8.

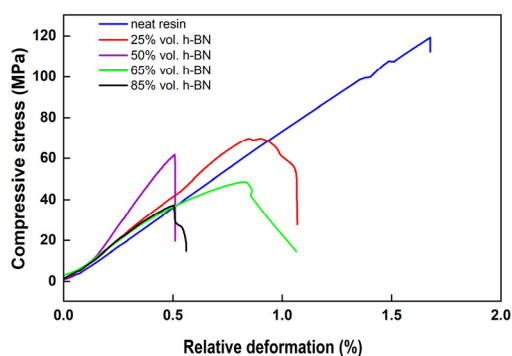


Figure 8. Dependence of compressive stress of relative deformation of samples.

As can be readily seen from the data, all composites as well as neat PR, demonstrate fragile behavior during compression. Introducing ceramic filler leads to a decreased ultimate deformation (increased brittleness) of the material and also increased rigidity (as indicated by Young's modulus). The overall effect is that the compressive strength of the composites under study, decreased almost steadily with an increase in the filler loading, indicating a dominant effect of the former factor. Nevertheless, even at a very-high filler loading (65 vol.%), the ultimate compressive strength was above 40 MPa, which is more than enough for the material to be machined into complex-shaped heatsink articles. A sharp decrease at 85 vol.% filler loading may once again be linked with increased porosity.

It should also be noted that Young's modulus of composites, throughout all the studied concentrations, was close to that of neat resin, which, in this case, should mean that composite mechanics in the elastic region are primarily defined by the matrix. The layered filler particles apparently do not contribute to the stiffness of the composite at low strains and influence mechanics at higher deformations due to porosity and its resistance to crack propagation.

4. Conclusions

h-BN/PR composites were obtained in a wide range of component ratios via solution mixing, vibrational milling and hot-compression molding. The thermal conductivity of the obtained materials varied in the range from 0.63 to 18.5 W·m⁻¹·K⁻¹ at filler loadings of 5 to 85 vol.%, respectively. Increased porosity is only significant above 80 vol.% loading, so the proposed technology is quite effective for manufacturing composites with extremely high filler loadings. The percolation threshold is not very pronounced, but lies in the range 25–30 vol.%. Reported data on thermal conductivity is significantly higher than published values for bulk BN/polymer composites, which can be explained by both high-filler loading and advantages of the proposed technology. This fact can be attributed to resin curing under pressure, ensuring the optimal level of adhesion on the matrix-filler interface, optimal filler particle size, as well as two-step mixing that enabled homogeneous dispersion of the filler.

Several models were considered to describe thermal conductivity in h-BN/PR composites. An isolated medium model is inadequate in this particular case, whereas the effective medium (Bruggeman) model, although hugely overestimates at higher concentrations, may be used as an approximation at concentrations up to 30 vol.%. The best fitting was achieved with the Agari–Uno model, using parameters of $C_1 = 0.7$ and $C_2 = 1.0$. Therefore, composite behavior, in this case, is best distributed with a mixed series-parallel model with filler particles prone to the formation of percolation-type networks.

Thermogravimetric analysis provided the evaluation of short-term degradation stability; it is sufficient for the use of manufactured composites in high-temperature power electronics (over 480 K). As thermal stability significantly improves with an increase of filler loading, it is very important for prospective applications to develop stable technologies for manufacturing materials with over 50 vol.% of h-BN.

The dielectric constant ranged from 5.6 to 4.2 for 85 and 5 vol.% respectively. As the difference in component values for ϵ_r is not very large, Maxwell–Garnett model, which is based on an isolated medium approximation, describes the obtained experimental values with high accuracy (but so does the rule of mixtures). Dielectric loss tangent $\tan \delta$ values are also small (0.015 to 0.055) and weakly frequency-dependent, at least in the 20 KHz–1 MHz range. Specific active resistance of the materials ranged from 17 to 140 M Ω . It is concluded that reported composites are applicable as dielectric heatsink materials for electronics. Mechanical properties (compression strength over 40 MPa at 65 vol.% h-BN) of the composites are sufficient for the manufacturing of complex-shaped articles via most conventional machining techniques.

Taking into account the excellent dielectric properties of the obtained h-BN/PR composites, the high-thermal stability both in inert and oxidative atmospheres, controlled anisotropy of thermal conductivity, as well as its high absolute values and relatively low density, shows that reported composites are promising for the application as components of heat-removal systems in electronic engineering and microelectronics. Composites may also be used to manufacture independent heat-dissipating elements (various heat exchangers), since they can be machined into complex shapes. Current research suggests that it is generally feasible to achieve even higher filler loadings in h-BN/polymer composites, as filler content above 60 vol.% enables to drastically increase thermal conductivity, thermal stability, and dielectric properties.

Author Contributions: Conceptualization, A.A.S., E.A.D. and V.M.S.; methodology, E.A.D. and I.M.K.; validation, I.M.K., E.V.M. and V.V.T.; formal analysis, E.A.D.; investigation, E.A.D. and I.M.K.; data curation, E.A.D.; writing—original draft preparation, E.A.D.; writing—review and editing, A.A.S., V.V.T. and E.V.M.; visualization, V.V.T., E.A.D.; supervision, E.A.D. and V.M.S. All authors have read and agreed to the published version of the manuscript.

Funding: This research received no external funding.

Data Availability Statement: The data presented in this study are available on request from the corresponding author.

Acknowledgments: The authors would like to declare their gratitude to V. Sapozhnikov for TGA measurements, and L.V. Kim of JSC “NIIgrafit” for thermal conductivity measurements.

Conflicts of Interest: The authors declare no conflict of interest.

References

1. Feng, C.P.; Yang, L.Y.; Bai, L.; Bao, R.Y.; Liu, Z.Y.; Yang, M.B.; Lan, H.B.; Yang, W. Recent advances in polymer-based thermal interface materials for thermal management: A mini-review. *Compos. Commun.* **2020**, *22*, 100528. [[CrossRef](#)]
2. Prasher, R. Thermal interface materials: Historical perspective, status, and future directions. *Proc. IEEE* **2006**, *94*, 1571–1586. [[CrossRef](#)]
3. Zhang, Y.; Ma, J.; Yang, J.; Pei, Q.X. Recent progress in the development of thermal interface materials: A review. *Phys. Chem. Chem. Phys.* **2021**, *23*, 753–776. [[CrossRef](#)] [[PubMed](#)]
4. Ma, H.; Gao, B.; Wang, M.; Yuan, Z.; Shen, J.; Zhao, J.; Feng, Y. Strategies for enhancing thermal conductivity of polymer-based thermal interface materials: A review. *J. Mater. Sci.* **2021**, *56*, 1064–1086. [[CrossRef](#)]
5. Tong, X.C. *Advanced Materials for Thermal Management of Electronic Packaging*; Springer Series in Advanced Microelectronics; Springer: Berlin/Heidelberg, Germany, 2011; Volume 30, pp. 1–616.
6. Cheng, S.; Li, Y.S.; Liang, J.J.; Li, Q. Polymer dielectrics and their nanocomposites for capacitive energy storage applications. *Acta Polym. Sin.* **2020**, *51*, 469–483.
7. Hansson, J.; Nilsson, T.M.J.; Ye, L.; Liu, J. Novel nanostructured thermal interface materials: A review. *Int. Mater. Rev.* **2017**, *63*, 22–45. [[CrossRef](#)]
8. Huang, C.; Qian, X.; Yang, R. Thermal conductivity of polymers and polymer nanocomposites. *Mater. Sci. Eng. R Rep.* **2018**, *132*, 1–22. [[CrossRef](#)]
9. Cevallos, J.G.; Bergles, A.E.; Bar-Cohen, A.; Rodgers, P.; Gupta, S.K. Polymer heat exchangers—History, opportunities, and challenges. *Heat Transf. Eng.* **2012**, *33*, 1075–1093. [[CrossRef](#)]
10. Vavidelu, M.A.; Kumar, C.R.; Joshi, G.M. Polymer composites for thermal management: A review. *Compos. Interfaces* **2016**, *23*, 847–872.

11. Pan, X.; Debije, M.G.; Schenning, A.P.H.J. High thermal conductivity in anisotropic aligned polymeric materials. *ACS Appl. Polym. Mater.* **2021**, *3*, 578–587. [[CrossRef](#)]
12. Krásny, I.; Astrouski, I.; Raudensky, M. Polymeric hollow fiber heat exchanger as an automotive radiator. *Appl. Therm. Eng.* **2016**, *108*, 798–803. [[CrossRef](#)]
13. Timbs, K.; Khatamifar, M.; Lin, W.; Antunes, E. Experimental study on the thermal performance of straight and oblique finned, polymer heat sinks. In Proceedings of the 22nd Australasian Fluid Mechanics Conference AFMC2020, Brisbane, Australia, 7–10 December 2020.
14. Marchetto, D.B.; Moreira, D.C.; Ribatski, G. A Review on polymer heat sinks for electronics cooling applications. In Proceedings of the 17th Brazilian Congress of Thermal Sciences and Engineering, Águas de Lindóia, SP, Brazil, 25–28 November 2018.
15. Chen, X.; Su, Y.; Reay, D.; Riffat, S. Recent research developments in polymer heat exchangers—A review. *Renew. Sustain. Energy Rev.* **2016**, *60*, 1367–1386. [[CrossRef](#)]
16. Agrawal, A.; Chandrakar, S.; Sharma, A. Mechanical and thermal behaviour of epoxy/hexagonal boron nitride/short sisal fiber hybrid composites. *IOP Conf. Ser. Mater. Sci. Eng.* **2020**, *840*, 012011. [[CrossRef](#)]
17. Yang, R.; Sheng, M.; Zhang, Y.; Gong, H.; Lin, X.; Pei, Y.; Zhang, X. Thermal and dielectric properties of epoxy-based composites filled with flake and whisker type hexagonal boron nitride materials. *High. Perform. Polym.* **2021**, *33*, 417–428. [[CrossRef](#)]
18. Zhang, Y.; Gao, W.; Li, Y.; Zhao, D.; Yin, H. Hybrid fillers of hexagonal and cubic boron nitride in epoxy composites for thermal management applications. *RSC Adv.* **2019**, *9*, 7388–7399. [[CrossRef](#)] [[PubMed](#)]
19. Zhou, W.; Zuo, J.; Zhang, X.; Zhou, A. Thermal, electrical, and mechanical properties of hexagonal boron nitride-reinforced epoxy composites. *J. Compos. Mater.* **2013**, *48*, 2517–2526. [[CrossRef](#)]
20. Gu, J.; Meng, X.; Tang, Y.; Li, Y.; Zhuang, Q.; Kong, J. Hexagonal boron nitride/polymethyl-vinyl siloxane rubber dielectric thermally conductive composites with ideal thermal stabilities. *Compos. Part. A Appl. Sci. Manuf.* **2017**, *92*, 27–32. [[CrossRef](#)]
21. Zhan, Y.; Long, Z.; Wan, X.; Zhan, C.; Zhang, J.; He, Y. Enhanced dielectric permittivity and thermal conductivity of hexagonal boron nitride/poly(arylene ether nitrile) composites through magnetic alignment and mussel inspired co-modification. *Ceram. Int.* **2017**, *43*, 12109–12119. [[CrossRef](#)]
22. Tang, Y.; Zhang, P.; Zhu, M.; Li, J.; Li, Y.; Wang, Z.; Huang, L. Temperature effects on the dielectric properties and breakdown performance of h-BN/epoxy composites. *Materials* **2019**, *12*, 4112. [[CrossRef](#)]
23. Fu, X.; Guo, Y.; Du, Q.; Guan, L.; He, S. Improved dielectric stability of epoxy composites with ultralow boron nitride loading. *RSC Adv.* **2019**, *9*, 4344–4350. [[CrossRef](#)]
24. Kochetov, R.; Andritsch, T.; Morshuis, P.H.F.; Smit, J.J. Effect of filler size on complex permittivity and thermal conductivity of epoxy-based composites filled with BN particles. In Proceedings of the 2010 Annual Report Conference on Electrical Insulation and Dielectric Phenomena, West Lafayette, IN, USA, 17–20 October 2010; p. 5723962.
25. Zhang, D.L.; Liu, S.N.; Cai, H.W.; Feng, Q.K.; Zhong, S.L.; Zha, J.W.; Dang, Z.M. Enhanced thermal conductivity and dielectric properties in electrostatic self-assembly 3D pBN@nCNTs fillers loaded in epoxy resin composites. *J. Mater.* **2020**, *6*, 751–759. [[CrossRef](#)]
26. Chiang, T.H.; Hsieh, T.E. A study of encapsulation resin containing hexagonal boron nitride (hBN) as inorganic filler. *J. Inorg. Organomet. Polym. Mater.* **2006**, *16*, 175–183. [[CrossRef](#)]
27. Yu, Z.; Wang, X.; Bian, H.; Jiao, L.; Wu, W.; Dai, H. Enhancement of the heat conduction performance of boron nitride/cellulosic fibre insulating composites. *PLoS ONE* **2018**, *13*, e0200842. [[CrossRef](#)]
28. Takahashi, S.; Imai, Y.; Kan, A.; Hotta, Y.; Ogawa, H. Dielectric and thermal properties of isotactic polypropylene/hexagonal boron nitride composites for high-frequency applications. *J. Alloys Compd.* **2014**, *615*, 141–145. [[CrossRef](#)]
29. Yuan, F.Y.; Zhang, H.B.; Li, X.; Li, X.Z.; Yu, Z.Z. Synergistic effect of boron nitride flakes and tetrapod-shaped ZnO whiskers on the thermal conductivity of electrically insulating phenol formaldehyde composites. *Compos. Part. A Appl. Sci. Manuf.* **2013**, *53*, 137–144. [[CrossRef](#)]
30. Wang, Z.; Liu, J.; Cheng, Y.; Chen, S.; Yang, M.; Huang, J.; Wang, H.; Wu, G.; Wu, H. Alignment of boron nitride nanofibers in epoxy composite films for thermal conductivity and dielectric breakdown strength improvement. *Nanomaterials* **2018**, *8*, 242. [[CrossRef](#)]
31. Moradi, S.; Calventus, Y.; Román, F.; Hutchinson, J.M. Achieving high thermal conductivity in epoxy composites: Effect of boron nitride particle size and matrix-filler interface. *Polymers* **2019**, *11*, 1156. [[CrossRef](#)]
32. Moradi, S.; Román, F.; Calventus, Y.; Hutchinson, J.M. Remarkable thermal conductivity of epoxy composites filled with boron nitride and cured under pressure. *Polymers* **2021**, *13*, 955. [[CrossRef](#)] [[PubMed](#)]
33. Tominaga, Y.; Hotta, Y.; Imai, Y. Effect of resin chemical structure on the dispersibility of hexagonal boron nitride. *Compos. Interfaces* **2020**, *27*, 967–975. [[CrossRef](#)]
34. Yi, L.; Conell, J.W. Advances in 2D boron nitride nanostructures: Nanosheets, nanoribbons, nanomeshes, and hybrids with graphene. *Nanoscale* **2012**, *4*, 6908–6939.
35. Guo, H.; Xu, T.; Zhou, S.; Jiang, F.; Jin, L.; Song, N.; Ding, P. A technique engineered for improving thermal conductive properties of polyamide-6 composites via hydroxylated boron nitride masterbatch-based melt blending. *Compos. Part. B Eng.* **2021**, *212*, 108716. [[CrossRef](#)]
36. Weng, Q.; Wang, X.; Wang, X.; Bando, Y.; Golberg, D. Functionalized hexagonal boron nitride nanomaterials: Emerging properties and applications. *Chem. Soc. Rev.* **2016**, *45*, 3989–4012. [[CrossRef](#)] [[PubMed](#)]

37. Jomon, J.; Elssa, G.; Prakashan, H.; Sabu, T.; Saithalavi, A. An overview of boron nitride based polymer nanocomposites. *J. Polym. Sci.* **2020**, *58*, 3115–3141.
38. Morchat, R.M.; Hiltz, J.A. A TGA study correlating polymer characteristics with smoke and flammability properties of polyester and phenolic resins. *Thermochim. Acta* **1991**, *192*, 221–231. [[CrossRef](#)]
39. Asim, M.; Saba, N.; Jawaid, M.; Nasir, M.; Pervaiz, M.; Alothman, O.Y. A Review on phenolic resin and its composites. *Curr. Anal. Chem.* **2018**, *14*, 185–197. [[CrossRef](#)]
40. Ghosh, B.; Xu, F.; Hou, X. Thermally conductive poly(ether ether ketone)/boron nitride composites with low coefficient of thermal expansion. *J. Mater. Sci.* **2021**, *56*, 10326–10337. [[CrossRef](#)]
41. Choupin, T.; Fayolle, B.; Renier, G.; Paris, C.; Senkin, J.; Brulem, B. Macromolecular modifications of the poly(etherketone ketone) copolymer (PEKK) in the state of melting. *Polym. Degrad. Stab.* **2018**, *155*, 103–110. [[CrossRef](#)]
42. Ko, T.H.; Hu, H.L.; Kuo, W.S.; Wang, S.H. Enhancing thermal conductivity and physical properties of phenol-formaldehyde resin by adding VGCF during pyrolysis. *J. Appl. Polym. Sci.* **2006**, *102*, 1531–1538. [[CrossRef](#)]
43. Liu, Y.; Nanwang, Y.L.; Lu, H.; Liu, J. Effect of boron nitride particle geometry on the thermal conductivity of a boron nitride enhanced polymer composite film. In Proceedings of the 25th International Workshop on Thermal Investigations of ICs and Systems (THERMINIC), Lecco, Italy, 25–27 September 2019; p. 8923441.
44. Wu, K.; Fang, J.C.; Ma, J.R.; Huang, R.; Chai, S.G.; Chen, F.; Fu, Q. Achieving a collapsible, strong and highly thermally conductive film based on oriented functionalized boron nitride nanosheets and cellulose nanofiber. *ACS Appl. Mater. Interfaces* **2017**, *9*, 30035–30045. [[CrossRef](#)] [[PubMed](#)]
45. Song, W.L.; Wang, P.; Cao, L.; Anderson, A.; Meziani, M.J.; Farr, A.J.; Sun, Y.P. Polymer/boron nitride nanocomposite materials for superior thermal transport performance. *Angew. Chem. Int. Ed.* **2012**, *51*, 6498–6501. [[CrossRef](#)] [[PubMed](#)]
46. Yu, C.; Zhang, J.; Tian, W.; Fan, X.; Yao, Y. Polymer composites based on hexagonal boron nitride and their application in thermally conductive composites. *RSC Adv.* **2018**, *8*, 21948–21967. [[CrossRef](#)]
47. Mehra, N.; Mu, L.W.; Ji, T.; Yang, X.T.; Kong, J.; Gu, J.W.; Zhu, J.H. Thermal transport in polymeric materials and across composite interfaces. *Appl. Mater. Today* **2018**, *12*, 92–130. [[CrossRef](#)]
48. Yu, L.; Gao, S.; Yang, D.; Wei, Q.; Zhang, L. Improved thermal conductivity of polymer composites by noncovalent modification of boron nitride via tannic acid chemistry. *Ind. Eng. Chem. Res.* **2021**, *60*, 12570–12578. [[CrossRef](#)]
49. Chen, L.; Li, K.; Li, B.; Ren, D.; Chen, S.; Xu, M.; Liu, X. Enhanced thermal conductivity of benzoxazine nanocomposites based on non-covalent functionalized hexagonal boron nitride. *Compos. Sci. Technol.* **2019**, *182*, 107741. [[CrossRef](#)]
50. Jiang, Y.; Shi, X.; Feng, Y.; Li, S.; Zhou, X.; Xie, X. Enhanced thermal conductivity and ideal dielectric properties of epoxy composites containing polymer modified hexagonal boron nitride. *Compos. Part. A Appl. Sci. Manuf. Solid-State* **2018**, *107*, 657–664. [[CrossRef](#)]
51. Lee, E.-S.; Kang, J.-G.; Kang, M.-K.; Kim, K.-H.; Park, S.-T.; Kim, Y.S.; Kim, I.; Kim, S.-D.; Bae, J.-Y. High thermal conductivity of boron nitride filled epoxy composites prepared by tin solder nanoparticle decoration. *Compos. Part. B Eng.* **2021**, *225*, 109264. [[CrossRef](#)]
52. Ge, M.; Zhang, J.; Zhao, C.; Lu, C.; Du, G. Effect of hexagonal boron nitride on the thermal and dielectric properties of polyphenylene ether resin for high-frequency copper clad laminates. *Mater. Des.* **2019**, *182*, 108028. [[CrossRef](#)]
53. Tang, X.; Guo, Y.; Liao, Z.; Fan, J.; Zhang, K.; Yang, Z. Synergistic enhancement of thermal conductivity between SiC and h-BN in MVQ-based composite. *Fuller. Nanotub. Carbon Nanostructures* **2019**, *27*, 434–439. [[CrossRef](#)]
54. Guzej, M.; Zachar, M.; Kominek, J.; Kotrbacek, P.; Brachna, R. Importance of Melt Flow Direction during Injection Molding on Polymer Heat Sinks' Cooling Efficiency. *Polymers* **2021**, *13*, 1186. [[CrossRef](#)]
55. Gu, J.; Lu, Z.; Wu, Y.; Guo, Y.; Tian, L. Dielectric thermally conductive boron nitride/polyimide composites with outstanding thermal stabilities via in-situ polymerization electrospinning-hot press method. *Compos. Part. A Appl. Sci. Manuf.* **2017**, *94*, 209–216. [[CrossRef](#)]
56. Yang, X.; Guo, Y.; Zheng, N.; Ma, T.; Tan, J. Self-healing, recoverable epoxy elastomers and their composites with desirable thermal conductivities by incorporating BN fillers via in-situ polymerization. *Compos. Sci. Technol.* **2018**, *164*, 59–64. [[CrossRef](#)]
57. Qin, M.; Xu, Y.; Cao, R.; Feng, W.; Chen, L. Efficiently controlling the 3D thermal conductivity of a polymer nanocomposite via a hyperelastic double-continuous network of graphene and sponge. *Adv. Funct. Mater.* **2018**, *28*, 1805053. [[CrossRef](#)]
58. Li, Z.; Wang, L.; Li, Y.; Feng, Y.; Feng, W. Carbon-based functional nanomaterials: Preparation, properties and applications. *Compos. Sci. Technol.* **2019**, *179*, 10–40. [[CrossRef](#)]
59. Jiang, F.; Zhou, S.; Xu, T.; Ding, P. Enhanced thermal conductive and mechanical properties of thermoresponsive polymeric composites: Influence of 3D interconnected boron nitride network supported by polyurethane@polydopamine skeleton. *Compos. Sci. Technol.* **2021**, *208*, 108779. [[CrossRef](#)]
60. Novokshonova, L.A.; Kudinova, O.I.; Berlin, A.A.; Grinev, V.G.; Nezhny, P.A.; Krashennnikov, V.G. Heat-Conducting Electrically Insulating Composite Material. Patent RU2643985C1, 16 January 2017.
61. Wang, Z.; Iizuka, T.; Kozako, M.; Ohki, Y.; Tanaka, T. Development of epoxy/BN composites with high thermal conductivity and sufficient dielectric breakdown strength part I—Sample preparations and thermal conductivity. *IEEE Trans. Dielectr. Electr. Insul.* **2011**, *18*, 1963–1972. [[CrossRef](#)]
62. Wereszczak, A.A.; Morrissey, T.G.; Volante, C.N.; Farris, P.J.; Groele, R.J.; Wiles, R.H. Thermally conductive MgO-filled epoxy molding compounds. *IEEE Trans. Compon. Packag. Manuf. Technol.* **2013**, *3*, 1994–2005. [[CrossRef](#)]

63. Bruggeman, D.A.G. Dielectric constant and conductivity of mixtures of isotropic materials [Original Title: Berechnung verschiedener physikalischer Konstanten von heterogenen Substanzen. I. Dielektrizitätskonstanten und Leitfähigkeiten der Mischkörper aus isotropen Substanzen]. *Annal. Phys.* **1935**, *24*, 636–679.
64. Nikoo, G.; Esfahani, S.; Armin, S.; Milad, M.; Hossein, N. The effect of filler localization on morphology and thermal conductivity of the polyamide/cyclic olefin copolymer blends filled with boron nitride. *J. Mater. Sci.* **2018**, *53*, 16146–16159.
65. Agari, Y.; Uno, T. Estimation on thermal conductivities of filled polymers. *J. Appl. Pol. Sci.* **1986**, *32*, 5705–5712. [[CrossRef](#)]
66. Dong, M.; Hou, G.; Zhang, J.; Liu, L.; Liang, G.; Hao, X.; Guo, Y.; Wang, M. Proposal and verification of thermal-conductive model of polymer nanocomposites. *Comp. Part. B Eng.* **2022**, *242*, 110033. [[CrossRef](#)]
67. Laturia, A.; Van de Put, M.L.; Vandenberghe, W.G. Dielectric properties of hexagonal boron nitride and transition metal dichalcogenides: From monolayer to bulk. *Npj 2D Mater. Appl.* **2018**, *2*, 6. [[CrossRef](#)]
68. Garnett, J.C.M. Colours in Metal Glasses and in Metallic Films. *Philos. Trans. Royal Soc. A Math. Phys. Eng. Sci.* **1904**, *203*, 385–420. [[CrossRef](#)]
69. Lucarini, V.; Peiponen, K.E.; Saarinen, J.J.; Vartiainen, E.M. *Kramers-Kronig Relations in Optical Materials Research*; Springer Series in Optical Sciences; Springer: Berlin/Heidelberg, Germany, 2005; Volume 110, pp. 1–162.
70. Shtansky, D.V.; Matveev, A.T.; Permyakova, E.S.; Leybo, D.V.; Konopatsky, A.S.; Sorokin, P.B. Recent Progress in Fabrication and Application of BN Nanostructures and BN-Based Nanohybrids. *Nanomaterials* **2022**, *12*, 2810. [[CrossRef](#)] [[PubMed](#)]

Disclaimer/Publisher’s Note: The statements, opinions and data contained in all publications are solely those of the individual author(s) and contributor(s) and not of MDPI and/or the editor(s). MDPI and/or the editor(s) disclaim responsibility for any injury to people or property resulting from any ideas, methods, instructions or products referred to in the content.